Eugene E. Lundquist

ARR Feb. 1943

NATIONAL ADVISORY COMMITTEE FOR AERONAUTICS

WARTIME REPORT

ORIGINALLY ISSUED

February 1943 as
Advance Restricted Report

PROGRESS REPORT ON FATIGUE OF SPOT-WELDED ALUMINUM

By H. W. Russell and L. R. Jackson
Battelle Memorial Institute

NACA

WASHINGTON

NATIONAL ADVISORY COMMITTEE FOR AERONAUTICS

ADVANCE RESTRICTED REPORT

PROGRESS REPORT ON FATIGUE OF SPOT-WELDED ALUMINUM

By H. W. Russell and L. R. Jackson

SUMMARY

This report contains a detailed account of approximately half of the work planned on Contract NAW 1659.

The work on this contract called for fatigue tests on three simple but basic types of spot-welded test pieces made from 24S-T alclad.

These were:

(1) A sheet lap joint to be loaded in repeated tension

(2) A stiffened panel to be loaded in repeated compression

(3) A nonstressed attachment joint, the sheet to be loaded in repeated tension but no load on the attachment

The fatigue tests were to be run on Krouse direct repeated stress machines. Since this type of fatigue machine is of recent design and has not had the history of service which, for example, characterizes the R. R. Moore type rotary-beam machines, it was felt desirable to spend considerable time in calibrating and studying the characteristics of the machine. In the course of this study, equipment utilizing SR-4 type strain gages was designed and constructed for studying the dynamic characteristics of the machine. The calibration of the machines and the stress-measuring equipment are described in the report.

Results obtained so far on lap joints can be summarized as follows:

1. Three typical types of failure were observed:

   (a) On all static tension tests and on some high-load fatigue tests, failure was by shear through the spots.

(b) On some high-load fatigue tests, spots failed by pulling buttons.

(c) On all low-load fatigue tests, failure was by cracks in the sheet originating at the spots and extending from spot to spot.

2. On static tension tests, the load-bearing ability in pounds per spot was the same for a spot spacing of 3/4 inch as for one of $1\frac{1}{4}$ inches; however, on fatigue tests, the 3/4-inch spacing was weaker in pounds per spot.

3. Tests run at different ratios of minimum to maximum stress indicated that the stress range allowable for a given life falls off as the mean stress is increased.

Results of tests on stiffened panels can be summarized as follows:

1. The stiffened panels consisted of hat-shaped stiffeners spot-welded to sheets and were so designed that failure was by buckling of the sheet rather than by Euler-column failure of the structure as a whole. The buckling produced tension-type failures in the spot welds.

2. Two thicknesses of stiffened sheet were investigated (0.051 in. and 0.032 in.) and two spot spacings ($1\frac{1}{4}$ in. and 3/4 in.). All tests so far were run at a ratio of minimum to maximum load of 0.25. Except at high loads, where the life was less than 100,000 cycles, the thick sheet withstood higher loads than the thin sheet and, in all cases, the test pieces with 3/4-inch spot spacing were stronger than those with $1\frac{1}{4}$-inch spot spacing.

3. At a life of 2×10^6 cycles, the 0.051 sheet withstood loads of about 62 percent of its static strength, and the 0.032-inch sheet withstood loads of 41 percent of its static strength. At a life of 100,000 cycles, the 0.032-inch panels had a strength of over 70 percent of the static strength while the 0.051-inch sheet withstood 68 percent of its static strength; thus, for relatively high loads, the thinner panels were as effective as the thicker ones.

No tests have yet been run on the unstressed attachments. The report contains a detailed account of methods of obtaining the results and a further discussion of their significance. The 24S-T alclad sheet used in this investigation was furnished by the Glenn L. Martin Co., through the courtesy of Mr. S. A. Gordon; hat-shaped stringer sections were furnished by the Curtiss-Wright Corporation through the courtesy of Mr. E. S. Jenkins; and the spot welding and X-ray examination of welds were done at the Welding Laboratory at Rensselaer Polytechnic Institute through the courtesy of Professor Wendell F. Hess.

I. FATIGUE TESTING AS APPLIED TO SPOT-WELDED SHEET

Under ideal conditions, an engineer would be able to compute exactly all stresses in a given structure, and it would then be possible to devise laboratory tests to select a material which could bear those stresses most efficiently. However, in the design of aircraft (as well as in most other design), there are many parts in which it is not possible to make an exact computation of service stresses and particularly of the alternating stresses which may be imposed during the life of a part. This situation would not be quite so serious if it were sufficient to supplement such design computations, as can be made, with static-load tests on selected structures. Unfortunately, no materials and structures have the same strength under alternating or vibrating loads as they do under steady load, and it is therefore necessary to develop information on the strength of materials and of structures made from these materials under dynamic loading.

It is the purpose of this investigation to develop this type of information on the use of spot welding as a means of fabricating aluminum sheet in aircraft design. In order to keep the investigation within reasonable limits, the work so far has been confined to the study of simple but basic design elements.

It is not to be expected that the data to be developed during this investigation will permit a designer to predict exactly the number of hours of flight an airplane, using spot-welded aluminum fabrication, will deliver; however, the data can reasonably be expected to indicate the relative merit of spot welds as compared with other types of fabrication. It is hoped that, in the hands of experienced designers, the data being developed here will enable the relatively untried spot-welding method of fabrication to find its proper place in aircraft construction without going through such a long period of expensive full-scale trial as might otherwise be necessary.

Even on a laboratory scale, it would be impractical to investigate all possible combinations of steady stress and alternating or fatigue-type stresses which might conceivably be placed on the structures under investigation. Fortunately, however, this is not necessary since the work of many previous investigators of fatigue strength of materials indicates that the behavior of a material for all possible combinations of simple stresses can be predicted with reasonable assurance if the behavior under a few strategically selected stress conditions is known.

One of the earliest fairly successful attempts to describe the effect a steady stress may have on the range of vibrating stress a material may carry indefinitely without failure was the Goodman (reference 1) diagram.

Figure 1 shows this diagram. In figure 1, the line OE is the axis of stress and OH is the axis of zero stress.

The line fc is drawn at 45° and the point c is located at the static ultimate stress Su. The line cd cuts the stress axis at a, a stress equal to 1/2 Su. The points d and f are located at plus and minus 1/3 Su, respectively. Points on the line ec represent values of mean stress.

The diagram states that when the mean stress is zero (point e) the alternating stress can vary from + 1/3 Su to - 1/3 Su indefinitely, while if the mean stress has a value j the alternating stress can vary only from k to l, a range less than for zero mean stress. At the point c (the ultimate strength) the allowable range of alternating stress is, of course, zero.

It has long been known that this diagram is only a crude approximation of experimental results, and recently J. O. Smith ("The Effect of Range of Stress on the Fatigue Strength of Metals," University of Illinois Bulletin No. 334 (1942)) has re-examined a large number of fatigue data from many sources, representing a wide range of materials and conditions. He has made some modifications in the method of representing data and has brought out some interesting relations between the effect of mean stress and the endurable range of alternating stress. Since some of his observations aid in the interpretation of data obtained here, the pertinent ones will be reviewed briefly. Smith uses several types of diagram, depending on the type of data to be analyzed. Figures 2(a) and 2(b) illustrate types pertinent to this investigation. Figure 2(a) states that, for shear fatigue stresses, the endurance limit for any mean stress $\overline{\tau_m}$ is constant and equal to the

endurance limit for completely reversed stress as long as Tmax (= Tm + Ta) Ty. Figure 2(b) states that for axial tension stresses the allowable alternating stress range diminishes linearly with the increase in mean stress. Actually, the majority of the data that Smith was able to gather lies above the line shown in figure 2(b), particularly at high values of mean stress. As will be shown later, the data obtained in this investigation can be represented by a diagram such as figure 2(b). This is consistent with Smith's further observation that when stress raisers such as notches (in this case, spot welds) are present, the data on fatigue in shear may also be represented by a diagram such as figure 2(b) instead of 2(a).

II. APPARATUS, CALIBRATION, AND TEST METHODS

Description of the Fatigue-Testing Machine

The tests to be reported here have been run on a Krouse fatigue-testing machine of 10,000-pounds-maximum load capacity. The machine can accommodate independently two specimens at one time. A photograph of the machine (fig. 3) shows one sample loaded in tension and indicates clearly the main features of loading.

The variable load is applied by the loading lever A actuated by the cam C, whose eccentricity on the driving pulley B can be adjusted to any desired value. The member transmitting the force to the specimen is guided by a parallelogram system of four steel-plate fulcrums D which produce straight-line motion and direct loading of the sample. The machine is a constant deflection type. The mean value of the load is adjustable by the loading screw E.

The static load value is obtained by measuring the bending of a fixed length of the loading lever A by means of the dial gage on the gage bar F. The relation between dial readings (relative to a reading with zero load) and load values is given by a calibration curve. This calibration was obtained (at the factory) by dead weights applied to the lower specimen holder for low loads and by a proving ring in place of the specimen for high loads. In practice, dial deflections are recorded for maximum and minimum loads as the cam B is rotated slowly by hand and the corresponding load values will be termed hereafter the "static load values."

The machine is equipped with two mechanical counters G, so geared to the driving shaft as to record one count for each hundred cycles of applied stress. The counters have a common drive but each may be reset to zero to correspond to the start of a run upon its particular sample. A cut-off H is designed to stop the motor and, hence, also the counters, when the load drops either by yielding or failure of the sample.

Important considerations in running any sample include: (1) clamping the sample so as to insure axial loading, (2) adjusting and determining the values of the loads applied, and (3) determining the number of cycles to failure. The precautions that have been taken in each of these three respects will now be discussed in some detail.

Clamping the Sample

(a) Tension Samples

Samples tested in tension were held in grips as shown in figure 3. In preparation, the sample was marked for the centers of the three bolt holes in each end by a steel template. The holes were then drilled 47/64 inch and the center hole at each end reamed to final size (3/4 in.). The sample was then mounted in the grips using only a center bolt at each end. With a moderate applied load (about 100 lb) on the sample, the remaining holes were reamed to size through the hardened sleeves in the grip bolt holes. After these holes were cleaned out, the remaining bolts were inserted. This procedure was designed to attain axial loading.

(b) Compression Samples

Figure 4 shows the compression grips used for the samples described later in this report. A is a platen to which was clamped the 5- by 5-inch surface ground-steel plate B. The small plates C and D were used to prevent slipping of the end of the sample. In practice, plate C was kept fixed so that, when the panel of the compression sample was against C, the center of mass of the sample was on the axis of loading. Plate D was tightened against the hat-shaped stiffener of each sample.

Shims (visible at E in fig. 4) were placed between A and B so that the face of B for the bottom compression plate was perpendicular to the leading axis. With a sample standing on the bottom plate, shims were adjusted for the upper grip so that its surface B rested evenly upon the top of the sample.

To avoid twisting the sample while adjusting the load, a rod was inserted in the disk A and held manually during the adjustment. Later, a clamp, designed to be fastened on the supporting columns, was constructed. This clamp may be seen above the upper compression grip in the photograph of figure 3.

Measuring the Load

A method of measurement of loads while the machine is running, using electrical resistance-type strain gages, was developed.

The principle of the measuring method is to apply an audio-frequency current to a Wheatstone-type bridge, one arm of which is an SR-4 type A1 gage mounted either on the test specimen in which it is desired to measure strains or on a weighbar in series with the specimen. The periodic strain in the test piece or weighbar varies the resistance of the gage. This variation in resistance modulates the audio-frequency signal being applied to the bridge. The bridge is balanced by means of a slide wire. A cathode-ray oscilloscope is used as a null-point indicator.

Figure 5 is a wiring diagram of the equipment, and figure 6 is a photograph of the assembly showing the various parts in place. In figure 5, the parts illustrated are as follows:

The Signal Source

A is a Hewlett Packard model 200 A audio oscillator. While this oscillator can provide frequencies from 35 to 35,000 cycles, it is being used at a constant frequency of 750 cycles. This frequency can be conveniently filtered so as to eliminate 60-cycle pickup.

B is a shielded isolating transformer with input and output impedances selected to match the oscillator and bridge, respectively. The transformer is a United Transformer Co. type LS141 transformer.

The Bridge

C is a dummy-type A1 gage mounted on a strip of material similar to the weighbar or test piece on which is mounted a similar gage D. These gages have an approximate resistance of 120 ohms and the dummy gage is mounted as close to the measuring gage as possible in order to secure temperature compensation. These two elements form two arms of the bridge. The other two arms are made up of resistance elements E, F, G, H, I, J, and K, which are selected to make, roughly, a 1:1 ratio with the SR-4 elements.

Resistances E, F, and R form a resistance combination of approximately 146 ohms. Resistances I, K, and the decade box J form a variable resistance combination which can be varied to suit the particular gages (C and D) being used, so that when the slide wire G is set at zero, the bridge is balanced for zero strain on D. The slide wire G is a Leeds & Northup Kolrausch type slide wire which is divided into 1000 divisions. The sensitivity of the bridge is such that one division on the slide wire corresponds to a resistance change of about 0.0009 ohm in gage D. This change in resistance is equivalent approximately to a strain of 4×10^{-6} inches per inch.

On account of stray capacitances, it is necessary to insert some capacity in one arm of the bridge in order to obtain a balance. This capacitance is shown as T in figure 1, and has a range of 40 to 1000 f. T is shown in arm C; however, it may be inserted in whatever arm that may be required to obtain a balance.

The Detector and Null-Point Indicator

The detector circuit includes a high-quality shielded-type 87A11 Stancor isolating transformer L, which matches the impedance of the bridge to the amplifier M. This amplifier is a David Bogen Co. type E14 amplifier with a variable gain from 0 to 125 db. The amplified signal is then passed through two filters, N and P, designed to select the band from 500 to 1000 cycles, and the filtered wave is shown on the oscilloscope.

N is a General Radio type 830-B, 500-cycle high-pass filter, and P is a General Radio type 930-E, 1000-cycle low-pass filter. Q is a DuMont type 168 oscillograph. All leads

connecting the various portions of the equipment are in shielded cables and the shields of all cables and transformers are grounded.

Several tests were made with the strain gage D on the sample itself and the dummy gage C on an unstrained sample nearby. It is time-consuming to use a new gage with each sample; moreover, a gage on the sample is subject to error at high loads when the sample is yielding. On the other hand, a weighbar in series with the sample offers difficulties in mounting the sample. Hence, some member of the machine itself, which would show appreciable strain proportional to the load, was sought.

A convenient arrangement proved to be this: Gage D was mounted on the plate fulcrum K (in fig. 3), while C was mounted at M. Thus, C served as temperature compensator to D and also, since M is in tension when K is in compression and vice versa, the arrangement offers reasonable sensitivity despite the relatively small strains in these plate fulcrums. It should be noted that the strain in gage D, owing to the bending of K, is largely compensated by a strain of gage C, owing to concurrent bending of M. Except at extremely low loads (less than 50 lb), the readings of the slide wire in the bridge circuit are linear with corresponding values of static load. Moreover, dynamic readings with this gage arrangement give values agreeing with those obtained by using a strain gage on the specimen itself. (The slight discrepancies at low loads can be eliminated by an arrangement wherein D consists of two strain gages mounted upon opposite sides of plate K and wired in series, while C is a similar arrangement upon plate M.)

One reason for the reproducibility (usually better than 1 percent) of dynamic load values obtained with the electric strain gages concerns the calibration method adopted. As an example, suppose it is desired to obtain dynamic values for some particular loading. The cam is turned by hand and readings of the dial gage and of the slide wire are recorded for maximum load, for minimum load, and for two or three loads in between these. This affords a calibration curve for the strain gage. Now the Krouse gage bar is removed, the motor is started, and dynamic values for maximum and minimum loads are read from the slide wire. The machine is now stopped and the calibration repeated. Thus, any shift in the strain-gage calibration caused, for example, by lack of complete temperature compensation, is noted. If such a shift is appreciable (which occurs only when the strain-gage circuit has been recently turned on and has not reached equilibrium), the readings are all repeated.

Many tests by the method described above indicate that the "dynamic throw" (max. load minus min. load when the machine is running) is about 15 percent greater than the "static throw" (difference between max. and min. loads when the cam is slowly turned by hand). That this throw increase is due to inertia of the moving loading lever was confirmed by tests with a series of strain gages mounted along the top of the loading lever (at N, O, P, etc. in fig. 3). The gage at N showed such a dynamic increase, the one at O showed little difference between dynamic throw and static throw, while gages at P, Q, and R showed static throws more than dynamic throws. These observations are readily understood if, because of inertia, the bending of the center line of the loading lever is along the lines sketched in figure 7. In such a case, the strain at N would be greater dynamically than statically while the strain at P, or Q, or R would be greater for static deflections. The point O is at the place where the strain is the same for both static and dynamic conditions.

All the tests that have been tried indicate that, with the calibration method used, strain gages on the plate fulcrums K and M are satisfactory. The graph plotted in figure 8 indicates that the dynamic throw is directly proportional to the static throw for a wide range in mean load and for specimens varying widely in stiffness. The points shown on the graph were obtained for (1) a stiffened aluminum panel (type D) loaded in compression, (2) a cast-iron pipe about 5 inches in diameter and 3/16 inch in wall thickness loaded in compression, (3) a steel plate about 15 inches long and 2 by 0.093 inch in cross section loaded in tension, and (4) a spot-welded 0.040-inch sheet of aluminum with welds 3/4 inch apart loaded in tension. It will be noted that the experimental points fall upon a straight line with consistency. A similar calibration curve was made for the right-hand side of the machine. It should be noted, since it does not appear on the graph, that the dynamic mean load had, within experimental error, the same value as the static mean load.

In view of the consistency of points for such plots, it seems justifiable to adopt a graph such as figure 8 as a calibration curve. Knowing the desired dynamic throw, the corresponding static throw is obtained from the calibration curve, and the loading is done statically.

Measuring the Number of Cycles to Failure

The fatigue-testing machine was originally equipped with electrically operated counters. Difficulties with these resulted in having them replaced by the mechanical counters already mentioned. These later counters are now operating satisfactorily.

The cut-off (which stops the machine when a test piece fails) consists of a microswitch operated by a change in the deflection of the center of the loading lever with a change in the maximum load. The motion available is only about 0.0035 inch for a change in maximum load of 100 pounds. With the present arrangement, the switch can be made to operate for a motion of 0.015 inch, which corresponds to a change in load of 430 pounds. The consistency of this "criterion of failure" is, of course, better than this in the sense that cut-off occurs at nearly the same (within about 80 lb) decrease in load for all samples.

The Routine Adopted for Fatigue Tests

In order to treat all samples consistently, a routine procedure of loading and checking samples has been established. Each sample is inspected for rough edges or visible flaws. The pertinent dimensions of each sample are recorded. From data obtained on previous tests, a load designed to give a desired point on the S-N curve is selected. Knowing the dynamic throw assigned, the static values at which the machine should be set are computed by using the dynamic throw calibration graph (fig. 8) for the particular machine. Using the calibration constant furnished with the machine, the dial readings to which the load is to be set are computed.

The sample is then placed in the clamps, with the precautions already noted, and the loading screw and the cam eccentricity are adjusted until the desired dial readings (within one-third dial division, corresponding to about 10 lb) are obtained. Now the machine is run for 1000 cycles, during which the mean load often decreases. The load is checked and, if necessary, restored to its original value. The machine is started and, after the cut-off adjustment has been checked, is left running.

All machines are checked frequently. A check includes counter-reading, reading of maximum and minimum load, a check on the cut-off adjustment, and careful visual examination of the sample.

III. MATERIALS, TEST PIECES, SPOT-WELDING DATA

EXAMINATION OF WELDS

Materials Used in Tests

Tests run so far have used 24S-T alclad sheet in three thicknesses: 0.032, 0.040, and 0.051 inch. Since, in all tests, primary interest is in the behavior of spot welds, the properties of the sheet material itself are not to be studied beyond securing assurance that the sheet is representative of its class of material. Pack compression tests on coupons cut from sheets used in making the samples described in this report are now being run at the Aluminum company laboratory through the courtesy of Mr. R. L. Templin.

Table I shows typical tension and compression data on 24S-T alclad taken from the Aluminum Company Research Laboratory, Technical Paper No. 6, published by the Aluminum company in 1942.

TABLE I. TYPICAL MECHANICAL PROPERTIES OF 24S-T ALCLAD

FROM ALUMINUM COMPANY TECHNICAL PAPER NO. 6

Sheet thickness (in.)	Tensile strength (lb/sq in.)	Yield strength 0.2 percent offset	Elongation 2 in.	Compression yield strength 0.2 percent offset
0.032	64,800	51,000	16.0	42,000
.051	66,900	51,800	19.0	41,200
.064	66,300	51,400	19.0	42,200

Test Pieces

Tension tests. - The lap-joint tension test pieces tested so far consisted of strips of 0.040-inch-thick 24S-T alclad sheet 9 inches long and 5 inches wide cut parallel to the direction of rolling and joined by a lap weld with an overlap of 1 inch.

Two weld spacings were investigated: 3/4 and $1\frac{1}{4}$ inches. The samples using the $1\frac{1}{4}$-inch spacing had four spots in the 5-inch width, while the samples using 3/4-inch spacing had six welds. In both cases the distance from the center of the single row of spot welds to the edge of the sheet was 1/2 inch. Figure 3 shows a six-weld test piece in the machine.

Compression tests. - The compression test pieces consisted of 24S-T alclad sheets $4\frac{1}{8}$ inches wide and either 0.032 or 0.051-inch-thick, spot-welded with two rows of spots to Curtiss-Wright SS-112-32 hat-shaped stringer sections. The stringer sections were made from 0.032-inch 24S-T alclad for all test pieces. Dimensions of the stringers are shown in figure 9. Two spot spacings were used for each sheet thickness. In one, the spot spacing was 3/4 inch except near the ends where the spots are located 1/8, 5/8, and $1\frac{1}{8}$ inches from the ends. In the second type, spot spacings were $1\frac{1}{4}$ inches except again near the ends where additional spots, spaced as above, were inserted. Figures 10(a), 10(b), 11(a), 11(b), 11(c), and 11(d) illustrate this type of specimen. After milling the ends square the test pieces with $1\frac{1}{4}$-inch spot spacing were $15\frac{7}{8}$ inches long, while the ones with 3/4-inch spacing were $15\frac{3}{4}$ inches long. Some engineering data on the stiffened panel sections are listed below.

Engineering Data on Stiffened Panel Sections

(1) Stringer Section Alone

Area, 0.165 square inch

Distance of centroidal axis from bottom edge of stringer, 0.485 inch

Moment of inertia around centroidal axis, 0.0723 inch^4

Radius of gyration around centroidal axis, 0.665 inch

(2) Stringer Spot-Welded to 0.032-Inch Sheet

Area, 0.309 square inch

Width between center line of spots, 2.7 inches

Distance of centroidal axis from face of panel, 0.284 inch

Moment of inertia around centroidal axis, 0.0617 inch^4

Radius of gyration around centroidal axis, 0.448 inch

(3) Stringer Spot-Welded to 0.051-Inch Sheet

Area, 0.395 square inch

Width between center line of spots, 2.7 inches

Distance of centroidal axis from face of panel, 0.238 inch

Moment of inertia around centroidal axis, 0.0620 inch^4

Radius of gyration around centroidal axis, 0.397 inch

TABLE II. WELDING CONDITIONS ON SPOT-WELD FATIGUE TESTS

Type of specimen	Thickness[3] (in.)	Secondary current[2]			Electrode tips		Electrode pressure				Surface treatment		
		Peak amperes	Time in milliseconds		Upper	Lower	Welding pressure (lb)	Forging pressure			Paint removal and degrease	Removing oxide	Shear strength single spot (lb)
			To peak	Time[1]				Maximum value (lb)	Time from peak current milliseconds				
									To start	To maximum			
Compression	0.032 sr 0.032 pl	30,400	16	62	2½" R dome	¼" x 10° flat	800	2400	12	110	Acetone trichloroethylene vapor	R.P.I. Sol #4	460
Compression	0.032 sr 0.051 pl	32,400	16	62	2½" R dome	¼" x 10° flat	800	2400	12	110	Acetone trichloroethylene vapor	R.P.I. Sol #4	505
Tension	0.040	41,800	18.5	67.5	4" R dome	4" R dome	1600	2400	9	22	Navy Specification C-67-C	R.P.I. Sol #10	602

[1]Total time from start of welding current until decay to 10 percent.

[2]Condenser discharge type of welder.

[3]sr = stringer, pl = panel.

Spot-Welding Data

The spot welding on all test pieces was done at Rensselaer Polytechnic Institute. Table II sumarizes their information on spot-welding conditions. A letter from Rensselaer Polytechnic Institute indicates that more details on the surface treatment of the sheet will be available in other reports.

Examination of welds. - An X-ray examination of all welds was conducted at Rensselaer Polytechnic Institute and indications were that all welds on test pieces reported here were sound.

A metallographic examination of some welds was made at Battelle; figure 12 illustrates typical weld structures. Measurements of several welds indicated that they had the following dimensions.

Type of weld	Diameter of melted zone in weld (in.)	Depth of penetration (percent)
0.040- to 0.040-inch sheet	0.22	50
0.032- to 0.032-inch sheet	0.155	70 to 80
0.051- to 0.032-inch sheet	0.160	60 to 70

IV. FATIGUE TESTS ON LAP-JOINT TENSILE TESTS

In section II, the method of making tension fatigue tests is described. Table III lists the types of sample used in tests reported here and static strengths of the various types. Static tension tests were run on a 20,000-pound Baldwin Southwark testing machine, using the same grips and mounting technique as for the fatigue tests.

Fatigue tests were designed to obtain data for plotting families of load-life curves at constant ratios (R) of minimum to maximum stress. Three ratios were used: $R = 0.25, 0.50,$ and 0.75.

It was noted in section II that, on the 10,000-pound Krouse-type fatigue machine, a drop in load of about 430 pounds was

required to actuate the cut-off mechanism which stops the machine and marks the end point of the test. This characteristic led to some difficulty in determining a proper criterion for failure; particularly at low loads, it was found that fatigue cracks started some time before they resulted in enough change in load to actuate the cut-off mechanism. On account of this, the test pieces were examined frequently during the progress of the test and the number of cycles at which cracks were first observed was noted; the number of cycles where the machine stopped was also recorded. It was not always possible to observe the beginning of the cracks; however, after considerable data had been accumulated, it was found that the ratio of the number of cycles for which cracks were first observed to the number for which cut-off occurred varied from 0.5 to 0.8. As might be expected, the higher values of this ratio are associated with the lowest number of cycles. For cut-off in less than 100,000 cycles, it was never possible to observe cracks before cut-off occurred.

Table IV summarizes fatigue results for the six-spot samples and table V summarizes those for the four-spot samples. The data are plotted in figures 13 and 14. In these figures points are designated by elongated crosses. Values for cut-off are plotted at the intersection of the cross and the length of the horizontal member of the cross is extended toward the axis of stress to the probable origin of cracking.

TABLE III. TEST PIECES AND STATIC STRENGTH VALUES ON LAP-WELD TENSION SAMPLES - ALL TEST PIECES WERE MADE FROM 0.040-INCH-THICK 24S-T ALCLAD SHEET

Sample number	Spot spacing (in.)	Number of spots	Rupture load (lb)	Rupture load (lb/spot)	Type of failure
3A-1	1¼	4	2400	600	Shear through spot
3A-9	1¼	4	2460	615	Do.
3A-27	3/4	6	3540	590	Do.
3A-30	3/4	6	3590	598	Do.

TABLE IV. TENSION FATIGUE TEST RESULT ON SPOT-WELDED LAP JOINTS IN 24S-T WELDED 0.040-INCH-SHEET THICKNESS SIX SPOTS SPACED 3/4 INCH

Sample number	Total maximum load (lb)	Maximum load (lb/spot)	Ratio $\frac{\text{Min. stress}}{\text{Max. stress}}$	Cycles to first observed crack	Cycles to failure	Type of break
3A-24	775	129	0.25		2,973,500	Fatigue cracks
3A-23	900	150	.25	135,900	257,400	Do.
3A-22	900	150	.25		638,000	Do.
3A-2	1050	175	.25		176,400	Do.
3A-29	1050	175	.25		261,000	Do.
3A-3	1200	200	.25	129,300	216,000	Do.
3A-1	1500	250	.25	94,200	126,600	Do.
3A-5	1800	300	.25		16,600	Shear and bonding
3A-4	2100	350	.25		3,400	Shear
3AB-11	900	150	.50		5,127,000	
3AB-12	1050	175	.50		1,039,400	Fatigue cracks
3AB-33	1350	225	.50	174,700	223,400	Do.
3A-31	1650	275	.50		31,200	Spots pulled
3A-32	1650	275	.50		87,000	Failure appears both as fatigue and tension
3A-26	1800	300	.50		68,000	
3A-28	2100	350	.50		31,700	
3AB-9	2400	400	.50		7,100	Shear type
3A-18	1200	200	.75		10,517,600	Fatigue cracks
3A-21	1350	225	.75		2,950,000	
3A-16	1500	250	.75		490,000	
3A-20	1650	275	.75		1,100,400	
3A-15	1800	300	.75	318,000	593,000	Fatigue cracks
3A-13	2100	350	.75		387,400	Do.
3A-8	2400	400	.75		143,000	Shear type
3A-14	2700	450	.75		205,800	Fatigue cracks
3A-17	3000	500	.75	88,000	107,600	Shear type
3A-19	3300	550	.75		400	Shear break

TABLE V. TENSION FATIGUE TEST RESULT ON SPOT-WELDED LAP JOINTS IN 24S-T WELDED 0.040-INCH SHEET THICKNESS

FOUR SPOTS SPACED 1½ INCHES

Sample number	Total maximum load (lb)	Maximum load (lb/spot)	Ratio Min. stress / Max. stress	Cycles to first observed crack	Cycles to failure	Type of break
3A-25	600	150	0.25		5,942,100	
3A-23	700	175	.25		1,309,200	Fatigue crack
3A-19	800	200	.25	420,000	779,600	Do.
3A-29	1000	250	.25	189,750	346,800	Do.
3A-14	1200	300	.25		25,200	Shear
3A-13	1500	375	.25		3,600	Do.
3A-15	1620	405	.25		1,000	Do.
3A-25 (reloaded)	1200	300	.25		113,000	Fatigue crack
3A-21	800	200	.50	515,500	964,500	Do.
3A-20	1000	250	.50	152,100	1,053,000	Do.
3A-18	1400	350	.50	60,000	70,200	Do.
3A-11	950	237	.75	1,453,700	2,984,600	Do.
3A-10	1000	250	.75		2,373,700	Do.
3A-24	1000	250	.75		3,200,000	Do.
3A-8	1100	275	.75	489,000	842,300	Do.
3A-7	1200	300	.75	1,152,300	1,761,600	Do.
3A-5	1400	350	.75	684,300	936,000	Do.
3A-2	1600	400	.75		533,300	Do.
3A-4	2000	500	.75	220,000	277,000	Do.
3A-6	2200	550	.75		41,200	Do.
3A-24 (reloaded)	1600	400	.75	200,000	1,380,000	Do.

The data presented above were obtained for three values of R. For use in design, it would be useful to have some information about the effect of a wider range in R and, particularly, to make some estimate as to the range in stress allowable for completely reversed stress. A modification of the methods used by Smith and described in section I allows such an estimate to be made.

Smith obtained the relation shown in figure 2 by using points on fatigue curves (such as those in figs. 13 and 14) at the endurance limit (i.e., for infinite life). Having the complete S-N curves, it is also possible to plot curves similar to Smith's curve for constant but finite lives. This has been done in figure 15, using constant life points on the curves in figures 13 and 14 to provide data for the curves in figure 15. Since Smith was interested in comparing a wide variety of materials, it was necessary for him to use dimensionless ratios of ultimate strengths for his coordinates. In this case, since only one material is involved, it is not necessary to use the ratio of mean steady stress to ultimate strength on the axis of abscissas; moreover, since the life for completely reversed stress is not only unknown but is the quantity desired, it is not possible to use the ratio Smith uses for ordinates. In view of this, the ordinate in figure 15 is the half range of alternating stress. The curves in figure 15 were obtained in the following manner. The points shown were computed from figures 13 and 14; these lines were drawn through the point representing static ultimate strength and as many points as possible on the curves of constant life. It will be noted that, in agreement with Smith's data, points for high values of mean stress lie above the lines so drawn. The intersection of those lines with the stress range axis is an estimate of the allowable values for completely reversed stress. While the extrapolation of the axis is beyond what good practice would recommend, the extrapolated results agree reasonably well with some reversed stress fatigue data on single spots obtained by Mr. Templin. While this agreement is not sufficient to inspire complete faith in the extrapolation shown in figure 15, the indications are that estimates so made will not be too far off.

The Mechanism of Fatigue Failures

During the course of testing, it was observed that there were three distinct types of failure, depending on the load and method of test. In static tests, failure always occurred by shear through

the spots. Figure 16 is an example of this type of failure. Tables IV and V describe the type of failure occurring in fatigue. It will be noted that, at high values of alternating stress, the fatigue failures either resembled the static failure (fig. 16) or "buttons" were pulled out at the spots as shown in figure 17. At lower stresses, failure was by propagation of cracks in the sheet between spots. These cracks originated at the top of each spot. Figures 18 and 19 illustrate this effect.

Microexamination of Failed Spots in Lap-Joint Tension Test Pieces

Metallographic work was carried out to secure information on the origin, location, and propagation of the fatigue cracks.

Specimen 3A-23 (see table V) loaded at 175 pounds per spot at 0.25 ratio was selected to show welds subjected to complete failure from fatigue cracking. Figure 20 shows four welds from this specimen, two of which were sectioned along the direction of application of stress and two perpendicular to this direction. Cracking was present only in those planes along the line of loading. The patterns of cracks shown in figure 21 were typical of those in all the tensile samples, in that the cracks were located at opposite sides and ends. Under especially severe loads, cracks sometimes started in the opposite direction from the normal break - presumably occurring after failure.

To study the point of fatigue-crack inception, a weld from specimen 3A-24 (see table IV) which had been under a low stress for nearly 3,000,000 cycles without showing any visible signs of failure was selected. Figure 22 indicates that cracks start at the point where the unmelted center aluminum coating projects into the weld zone. Although piping and inclusions sometimes were found in this area (fig. 23), the particular welds in figure 22 are very clean and show little evidence of these. Thus, failure probably occurred through the notch caused by the termination of the two sheets in the weld making a fatigue nucleus at this point. After starting, the cracks propagated through the dendritic region out to the edge of the sheet perpendicular to the weld axis.

TABLE VI. STATIC COMPRESSION TESTS ON STIFFENED PANEL SECTIONS

Specimen number	Panel thickness (in.)	Spot spacing (in.)	Load at which buckling starts (lb)	Maximum load before failure (lb)	Number of buckling waves
A-9	0.032	3/4	2500-3000	9,020	4
B-3	.032	1½	3000	8,350	4
C-8	.051	3/4	5020	11,720	3
D-10	.051	1½	4000	9,520	3

The results of microexamination of failures in spot welds in lap joints in tension can be summarized by saying that no evidence was found in which the metallurgical constituents or structure of the weld had any great influence on the type of failure; that is, in all cases, failure appeared to be associated with the notch as a notch rather than the type of metal structure.

V. COMPRESSION FATIGUE TESTS ON STIFFENED PANEL SECTIONS

The stiffened panel sections are described in detail in III. They consist of Curtiss-Wright SS-112-32 hat-shaped stringers made from 0.032-inch 24S-T alclad spot-welded to either 0.032- or 0.051-inch 24S-T alclad sheet.

Table VI identifies the test pieces and summarizes the results of static tests.

From table VI, it is evident that the buckling pattern is not dependent on the spot-weld spacing for the two spacings used. Observation of both the static and the fatigue tests did not detect any tendency to buckle between welds. The half-wave length of the buckling pattern in the 0.032-inch panels was about 2 inches, while that in the 0.051-inch panels was about 2.65 inches. In the 0.051-inch panels, the half-wave length was almost equal to the distance between rows of spots. During the fatigue tests, the buckling pattern was observed stroboscopically and found to have the same pattern as on the static tests.

TABLE VII. COMPRESSION FATIGUE RESULTS ON 0.051-INCH 24S-T ALCLAD STIFFENED PANELS

Sample number	Maximum load (lb)	Cycles to failure	Ratio $\frac{\text{Minimum load}}{\text{Maximum load}}$	Spot spacing (in.)
C9	9350	11,700	0.175	3/4
C3	8500	169,800	.25	3/4
C4	8275	220,000	.170	3/4
C2	7626	263,700	.173	3/4
C6	7600	217,000	.164	3/4
C10	6900	165,000	.162	3/4
C5	6750	1,500,000	.250	3/4
C7	6500	4,000,000 (did not fail)	.200	3/4
D7	7250	900	.25	1¼
D2	7000	66,000	.25	1¼
D1	7000	66,800	.25	1¼
D8	6500	290,000	.25	1¼
D4	6500	42,600	.25	1¼
D3	6500	22,000	.25	1¼
D6	6250	638,000	.25	1¼
D9	6000	10,558,600	.25	1¼

TABLE VIII. COMPRESSION FATIGUE RESULTS ON 0.032-INCH 24S-T ALCLAD STIFFENED PANELS

Sample number	Maximum load (lb)	Cycles to failure	Ratio $\frac{\text{Minimum load}}{\text{Maximum load}}$	Spot spacing (in.)	Remarks
A6	7218	63,600	0.25	3/4	
A10	6498	144,000	.25	3/4	
A3	6000	167,900	.25	3/4	
A5	5496	252,900	.25	3/4	
A2	4500	812,400	.25	3/4	
A7	3996	815,200	.25	3/4	
A8	3498	20,000,000	.25	3/4	Did not fail
A8 (reloaded)	3996	1,202,420	.25	3/4	
B9	5500	3,140	.25	1¼	
B5	5000	58,000	.25	1¼	
B10	4450	104,000	.25	1¼	
B2	4080	62,000	.25	1¼	
B6	3980	309,600	.25	1¼	
B1	3525	1,530,000	.25	1¼	
B7	3500	31,200	.25	1¼	
B8	3300	2,127,600	.25	1¼	
B4	2550	22,000,000	.25	1¼	Did not fail
B4 (reloaded)	3500	7,500,000	.25	1¼	

The fatigue data on the 0.051-inch stiffened panels are summarized in table VII, and those for the 0.032-inch panels in table VIII. The data for all four types are plotted in figure 24.

In table VII, it will be noted that ratios of minimum to maximum stress in the C-type specimens are not constant. Some of these specimens were run shortly after the Krouse machine was delivered and before it was found necessary to calibrate the machine dynamically. Thus, the points shown as curve C in figure 24 do not properly belong together. However, it is evident that the slope of C will not be far different from that for D, and that the curves for the 0.051-inch panels are much shallower than those for the 0.032-inch panels. It will also be noted that, for a given load, the samples with the 3/4-inch-spot spacing had longer lives than those with 1¼-inch spacing.

The ordinates in figure 24 are total compression load and the relation between this load and the tension stresses on any spot is not linear. The tension stress on the spots is very low until buckling starts; at that point tension stresses become appreciable and increase more rapidly for the thick sheets than for the thin one for further increases in load. Near the endurance limit the 0.051-inch panels have a fatigue strength about 62 percent of their static strength, while on the thin panels the fatigue strength is only about 41 percent. At higher loads, and for shorter lives, the thin panels are more efficient than the thick ones. For example, at a life of 100,000 cycles, the A samples (3/4 in. spacing, 0.032 in. panel) have a fatigue strength over 70 percent of their static strength, while the D samples (1¼ in. spacing, 0.051 in. panel) have a fatigue strength about 68 percent of the static strength.

In view of these results, there would appear to be arguments in favor of the use of thin panels under some conditions. Another consequence of the test was the observation that there were no fatigue failures at loads under those producing buckling. Another way of stating this observation is that when buckling is observed, fatigue failures may be expected. This state of affairs is probably a consequence of the spot spacing and type of buckling. If the spots had been far enough apart so that buckling occurred between spots, it is quite probable that buckling would not be so strongly associated with fatigue failures.

Further conclusions may be justified when other stress ratios have been explored.

The Mechanism of Fatigue Failures in Stiffened Panels Under Compression and Microstructure of Failed Spots

Figures 9(a) to 11(b) show typical fatigue failures in the four types of stiffened panels. In all cases, the first spot was a tension type. Usually the failure of one spot was followed closely by a tearing failure in the spots immediately adjacent.

A variety of crack patterns was obtained in the sectioning of welds in the stiffened compression samples. However, inception of cracks occurred in the same location as those in the tensile specimens - that is, at the point at which the alclad projects into the weld zone. It should be kept in mind in examining the micrographs in this section that they do not include the first spot to break, since this spot was always damaged too much for examination. Thus, cracks observed are not necessarily typical of the first spot to fail.

For welds, sectioned in the direction of stress application, which are adjacent to the first failure in the compression sample, cracks appeared both at the point of alclad projection in the direction of the sheet surface and from the same point in the main axis of the spot weld. Figures 25 and 26(a) show the type of failure occurring in the same spot. Figure 25 is also of interest in showing a crack starting from a scratch in the sheet.

For welds sectioned normal to the direction of stress, the failure occurred by tearing through the main axis of the weld (fig. 26(b)). For spots sectioned in the same manner, but having a weld spacing of 3/4 inch rather than 1¼ inches, discontinuous cracks were found parallel to the main axis of the weld but occurring in the dendritic rather than the equiaxed area (fig. 27). These cracks appeared to have been caused by fatigue rather than by a heavy rupturing load as in figure 26(b).

Battelle Memorial Institute,
Columbus, Ohio.

REFERENCE

1. Goodman, John: Mechanics Applied to Engineering. Longmans, Green & Co., (London), p. 635.

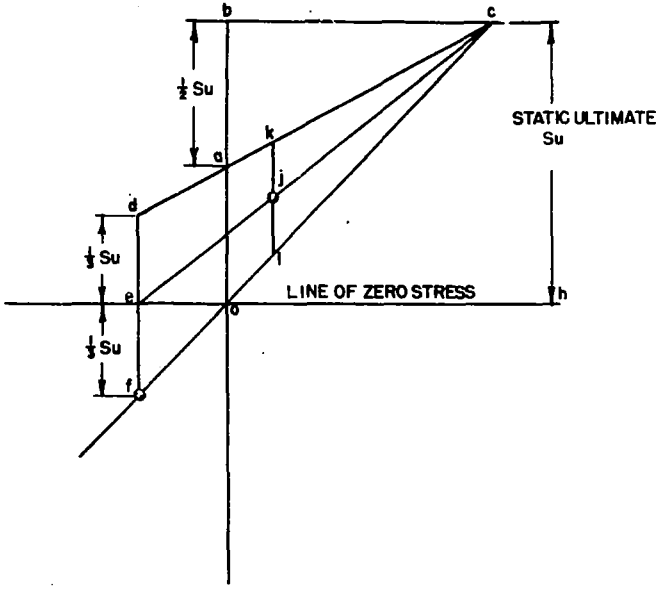

FIG. 1 – GOODMAN DIAGRAM SHOWING EFFECT OF MEAN STRESS ON RANGE OF STRESS AT ENDURANCE LIMIT.

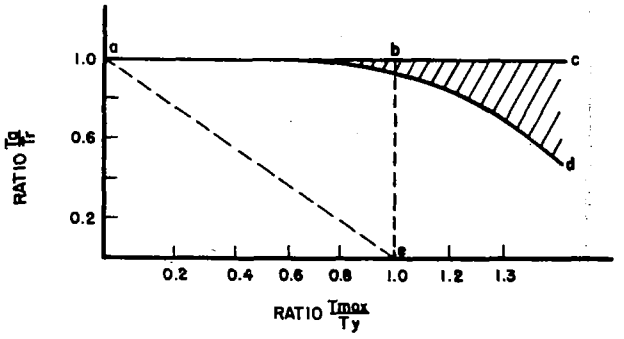

FIG. 2a – TYPE 1 SMITH DIAGRAM. Ty = YIELD STRENGTH IN SHEAR.
Tmax = MAXIMUM SHEAR STRESS. Ta = ½ ALTERNATING STRESS RANGE AT ENDURANCE LIMIT AND FOR MAXIMUM STRESS Tmax.
Tr = ½ ALTERNATING STRESS RANGE FOR COMPLETELY REVERSED STRESS.

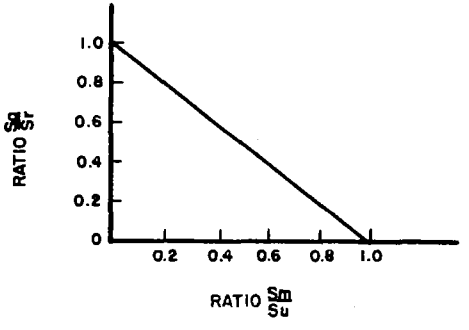

FIG. 2b – TYPE 2 SMITH DIAGRAM.
Sm = MEAN STEADY STRESS IN TENSION
Su = ULTIMATE TENSILE STRESS.
Sa = – ALTERNATING STRESS RANGE AT MEAN STRESS Sm.
Sr = – ALTERNATING STRESS RANGE FOR COMPETELY REVERSED STRESS.

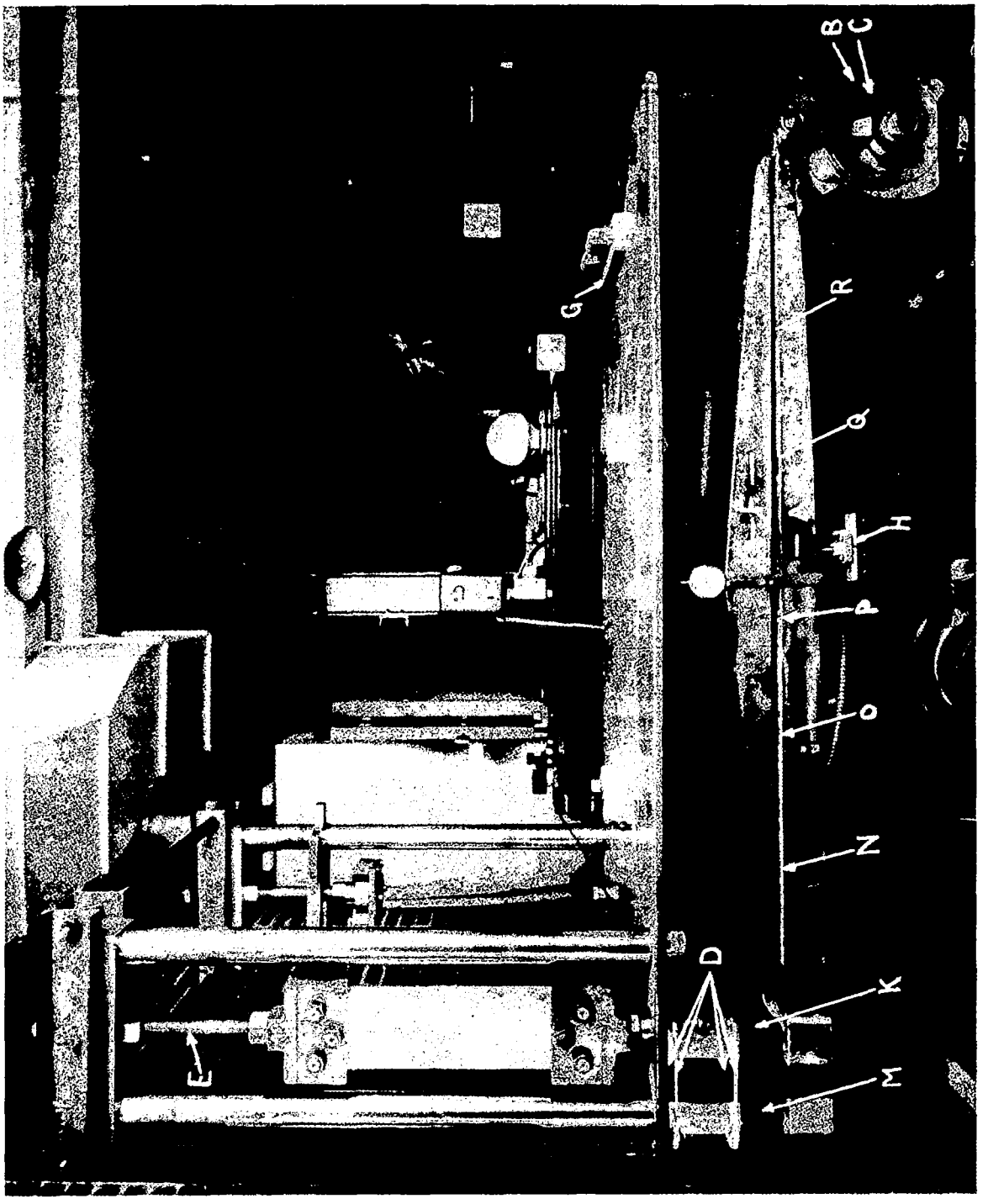

Figure 3. The Fatigue Testing Machine.

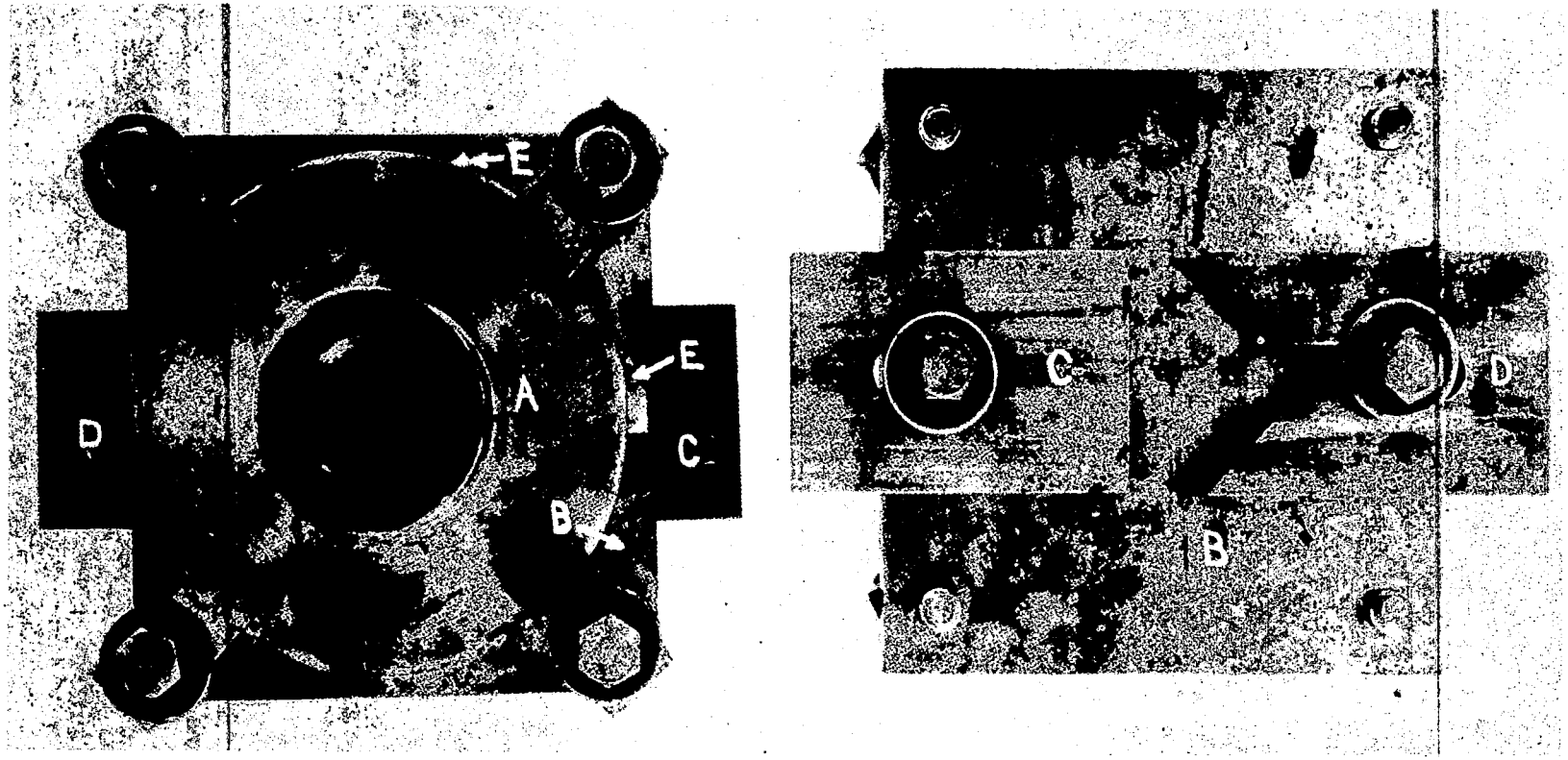

Figure 4. Grips for compression samples.

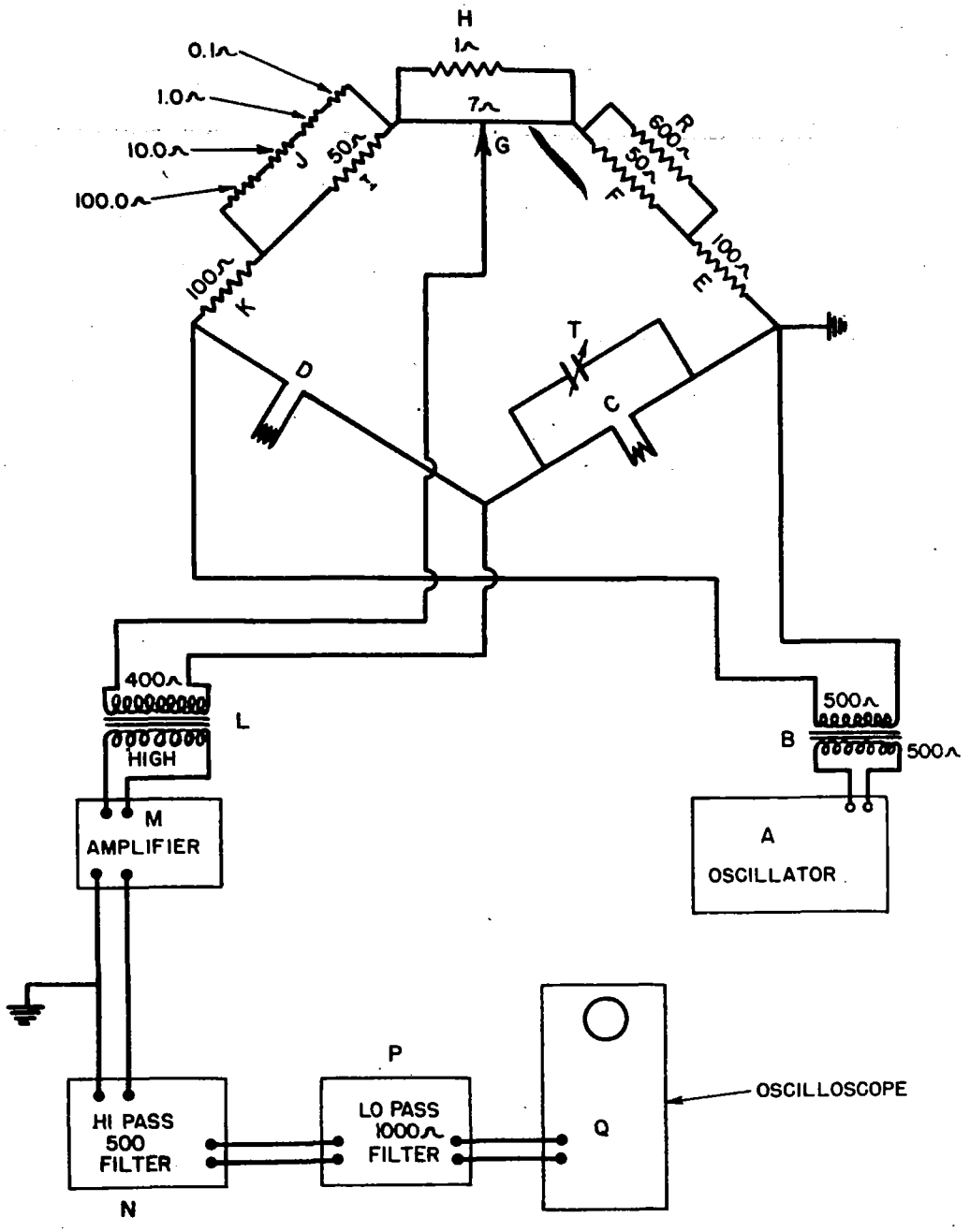

FIGURE 5-WIRING DIAGRAM OF STRAIN MEASURING BRIDGE

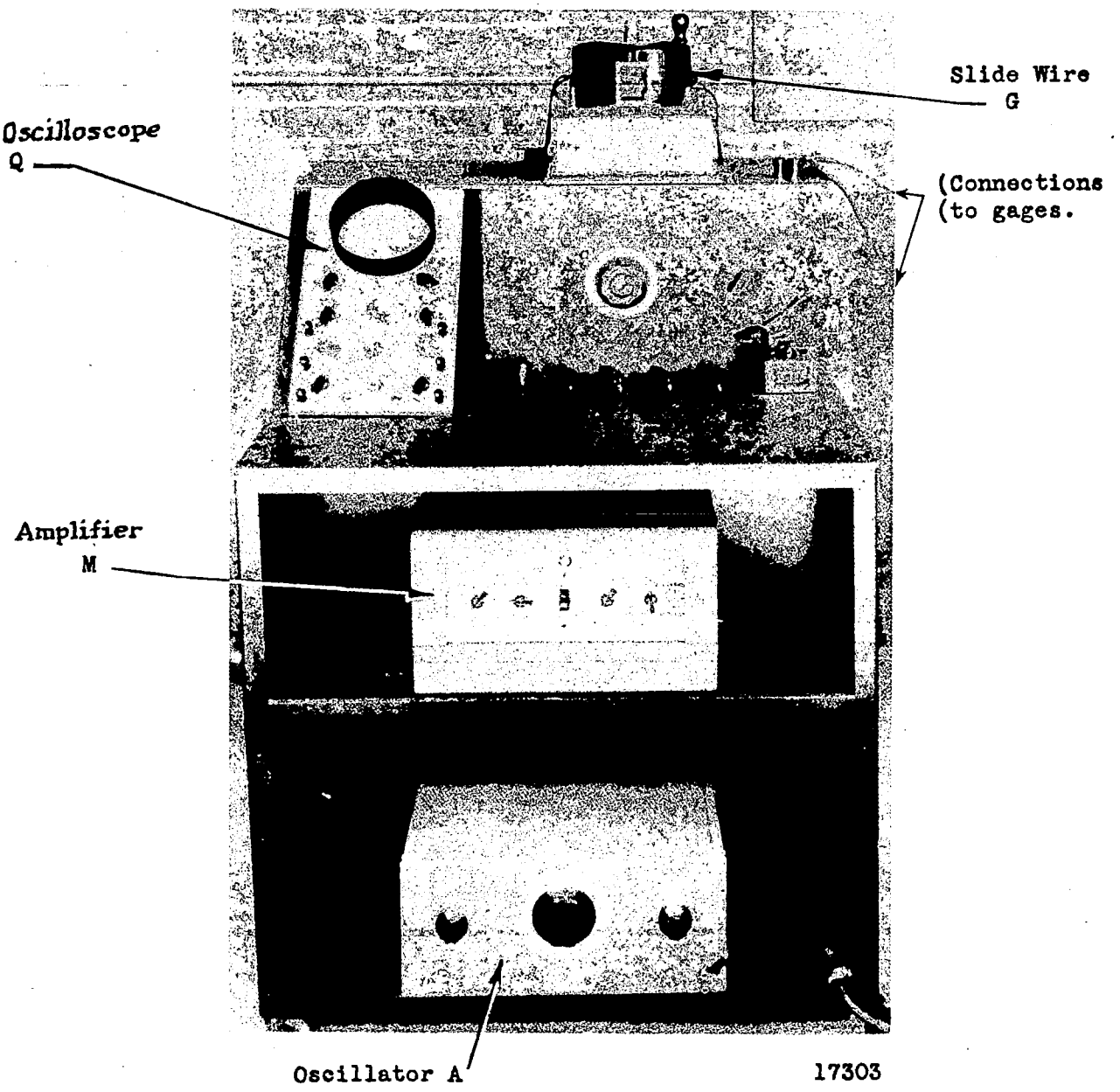

Figure 6.

Photograph of strain analysis equipment for use in making dynamic measurements with SR4 strain gages.

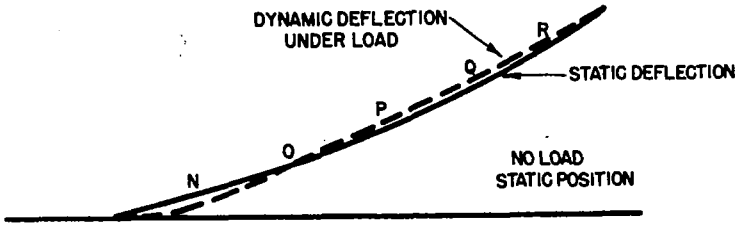

FIG. 7—DEFLECTION OF CENTER LINE OF LOADING LEVER (THE DEFLECTION IS GREATLY EXAGGERATED TO INDICATE THE EFFECT OF INERTIA. POINTS N,O,P,Q,R ARE POINTS OF ATTACHMENT OF STRAIN GAGES MENTIONED IN THE TEXT.)

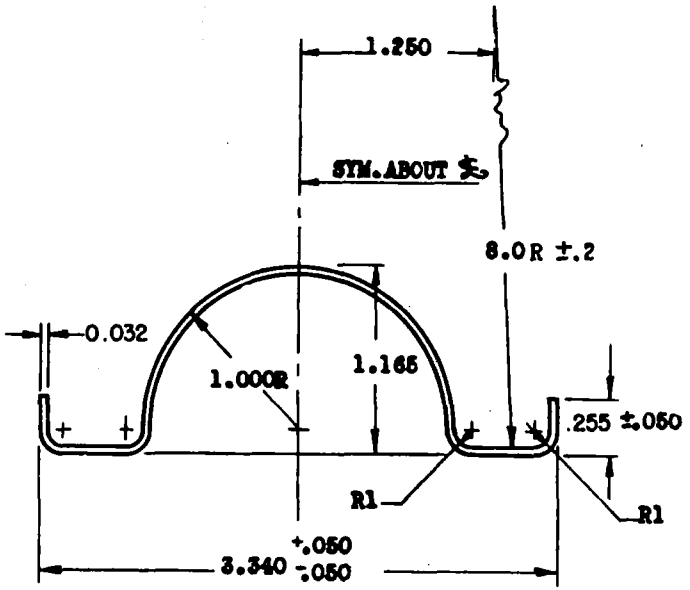

Figure 9.

Dimensions of Curtiss-Wright hat shaped stiffener.

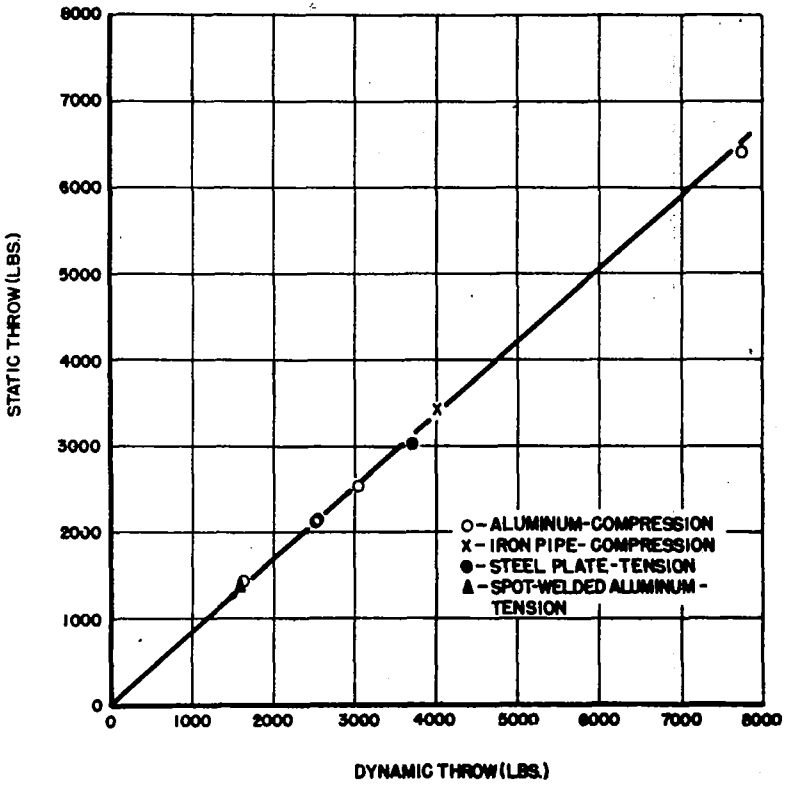

FIG. 8 - CALIBRATION FOR DYNAMIC THROW (LEFT HAND SIDE - MACHINE P-18)

18243

NACA

Figs. 7, 8, 9

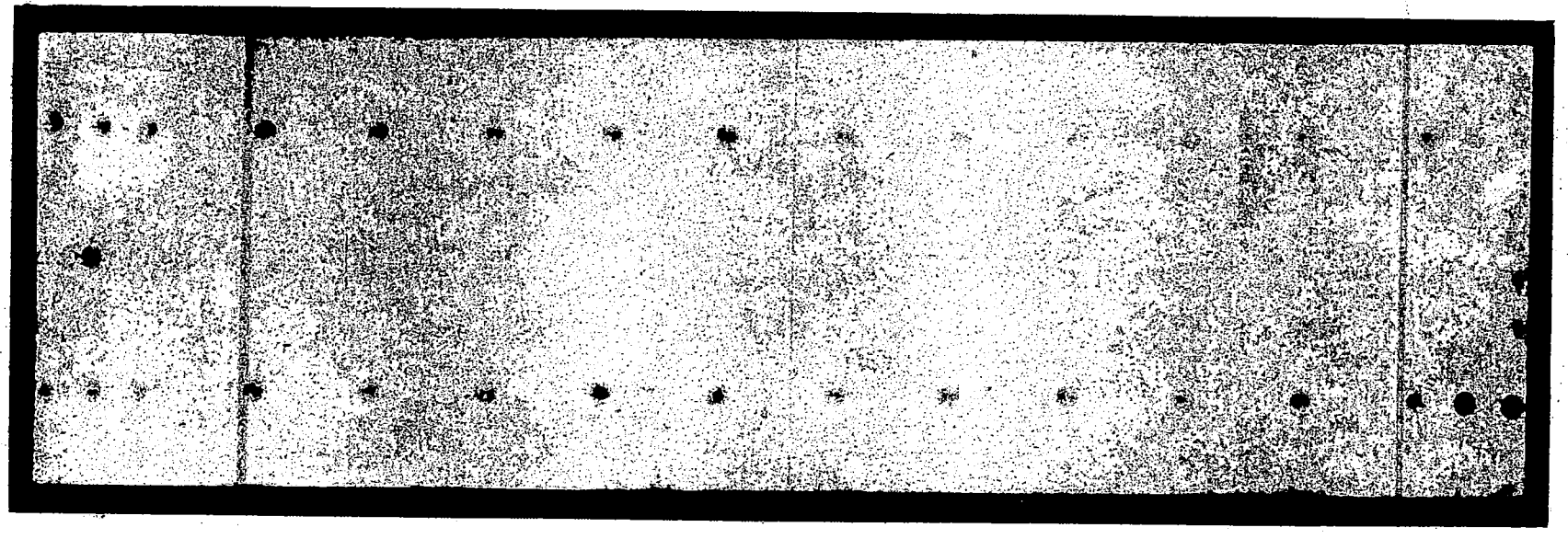

Figure 10a.- Back view B-Type compression sample loaded at 3980 lb and failing at 309,600 cycles.

$\frac{1}{2}$X

NACA
Figs.10a,b

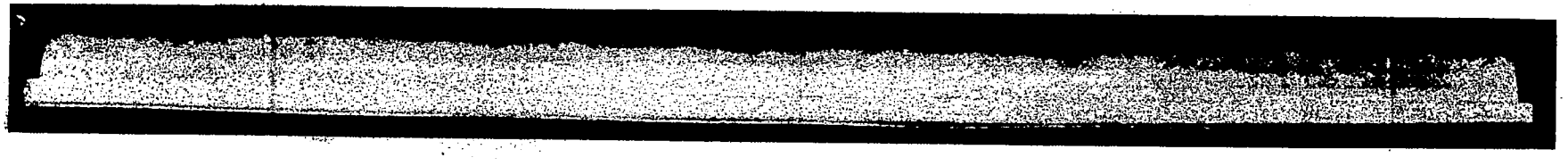

Figure 10b.- Side view.

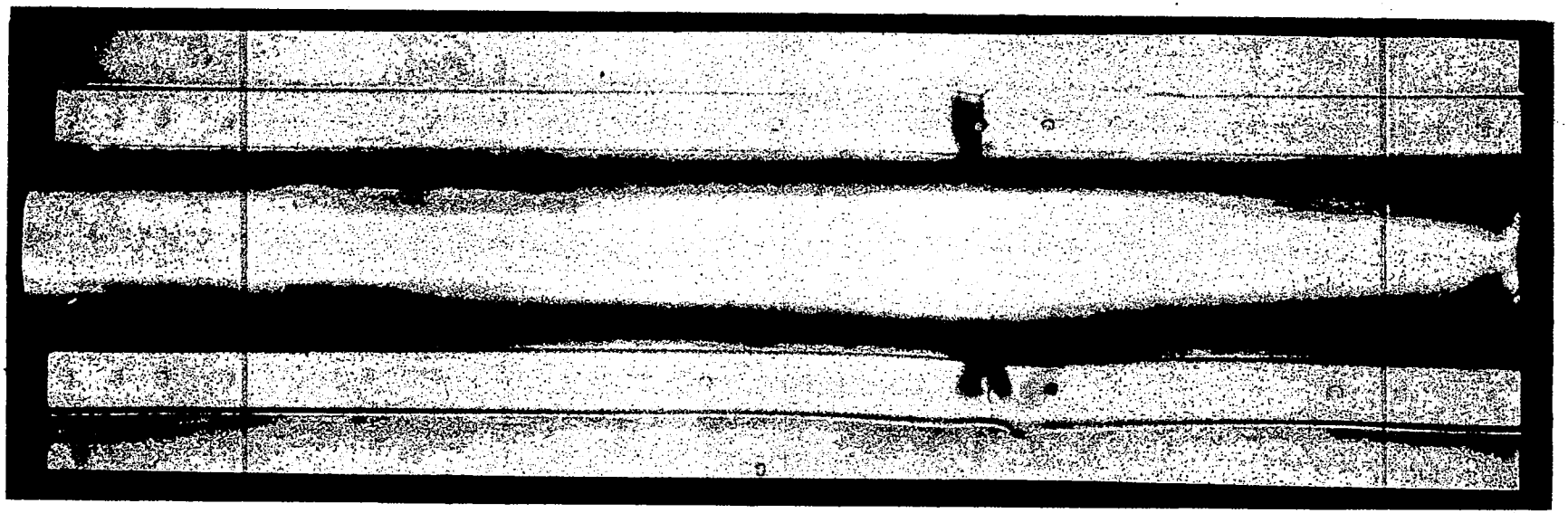

Figure 11a.- Front view C-Type compression sample loaded at 9350 lb and failing at 11,700 cycles.

$\frac{1}{2}$ X

NACA Figs. 11a,b

Figure 11b.- Side view.

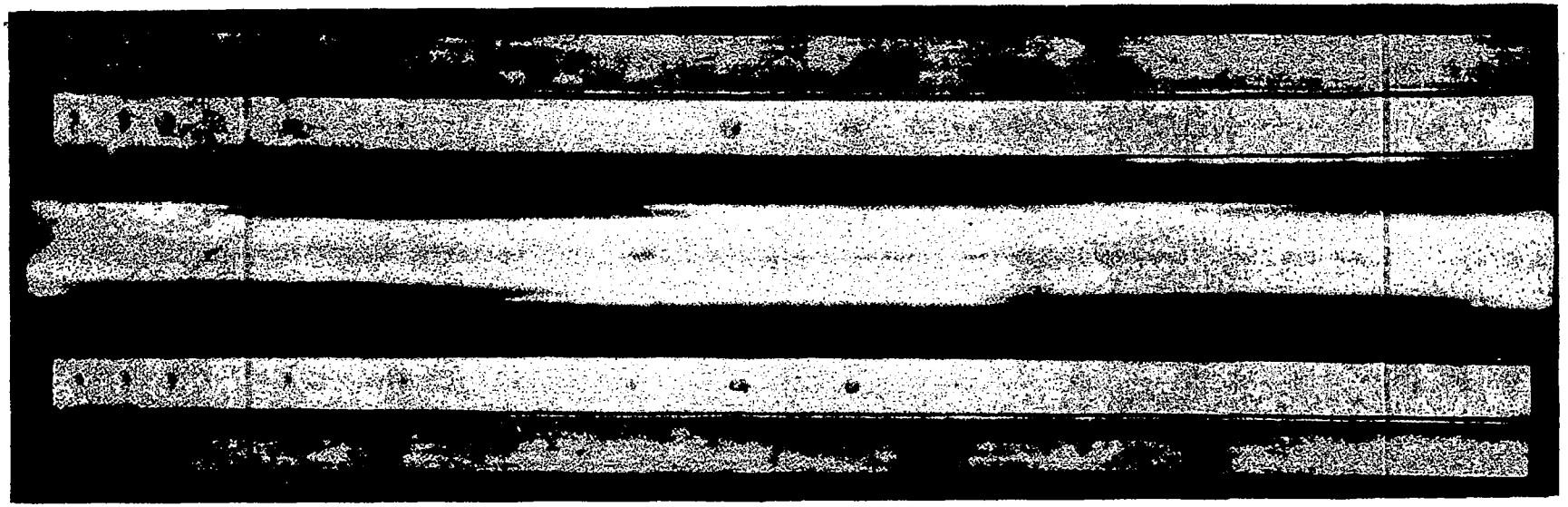

Figure 11c.- Front view D-Type sample loaded at 7000 lb and failing at 66,800 cycles.

$\frac{1}{2}$ X

NACA
Figs. 11c,d

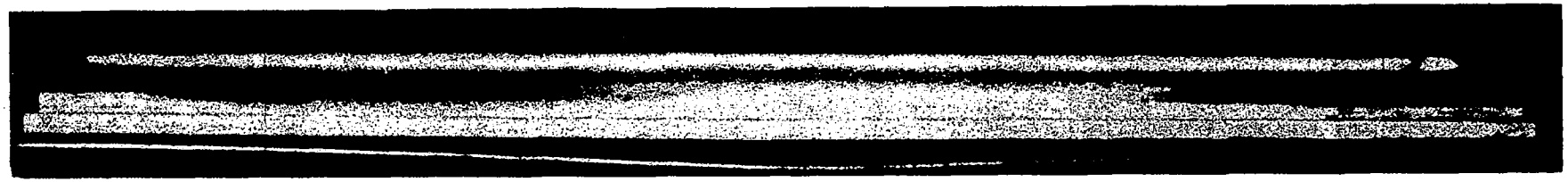

Figure 11d.- Side view.

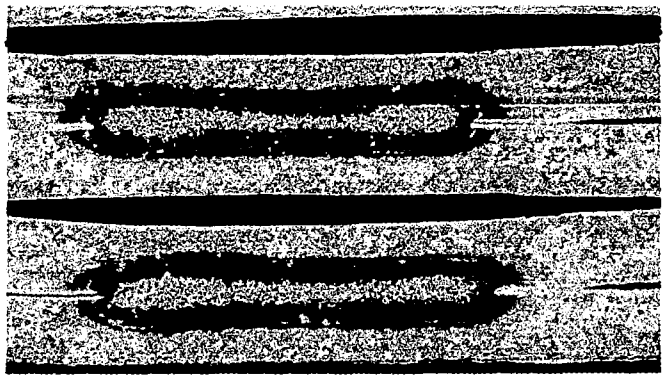

18274
10 X (a)

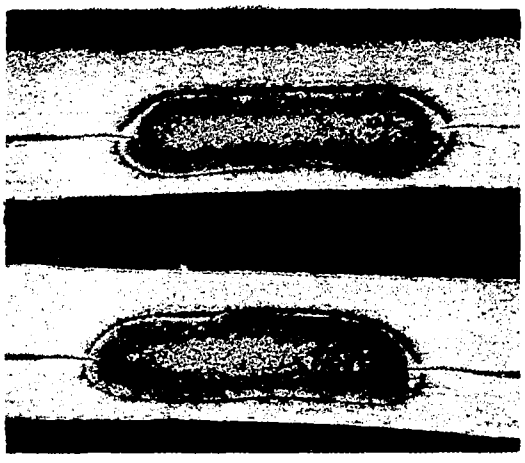

Kellers Etch
18275 (b)
10X

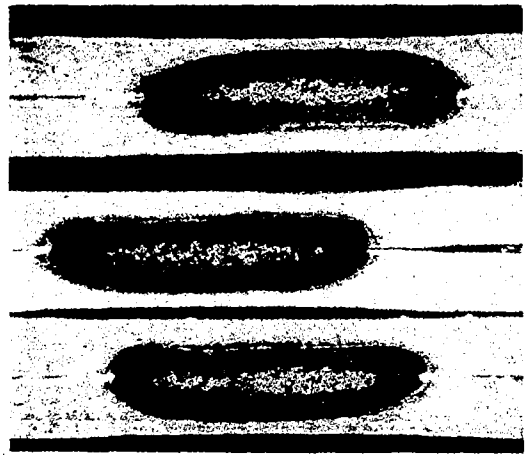

18276 (c)
10X

Figure 12.

Illustration of representative spotwelds. Original samples before testing:

(a) 0.040" - 0.040" Tension Sample
(b) 0.051" - 0.032" Compression Sample
(c) 0.032" - 0.032" Compression Sample

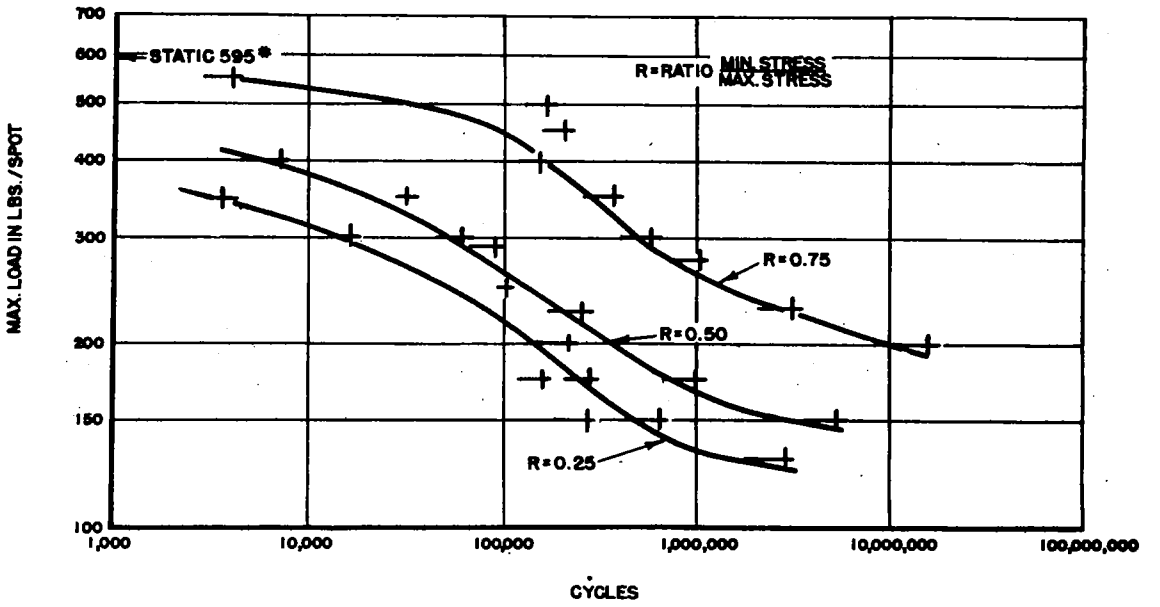

FIG. 13 – TENSION FATIGUE 0.040" ALCLAD SHEET 6 SPOTS SPACED $\frac{1}{2}$".

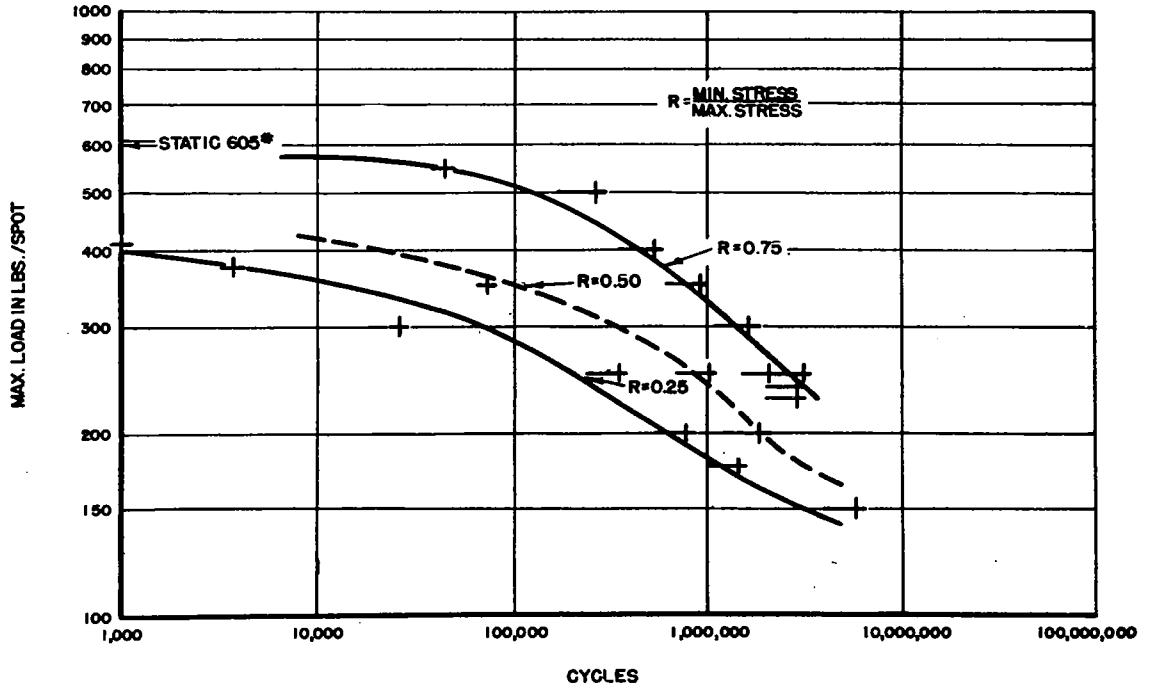

FIG. 14 – TENSION FATIGUE 0.040 ALCLAD SHEET 4 SPOTS SPACED 1$\frac{1}{2}$".

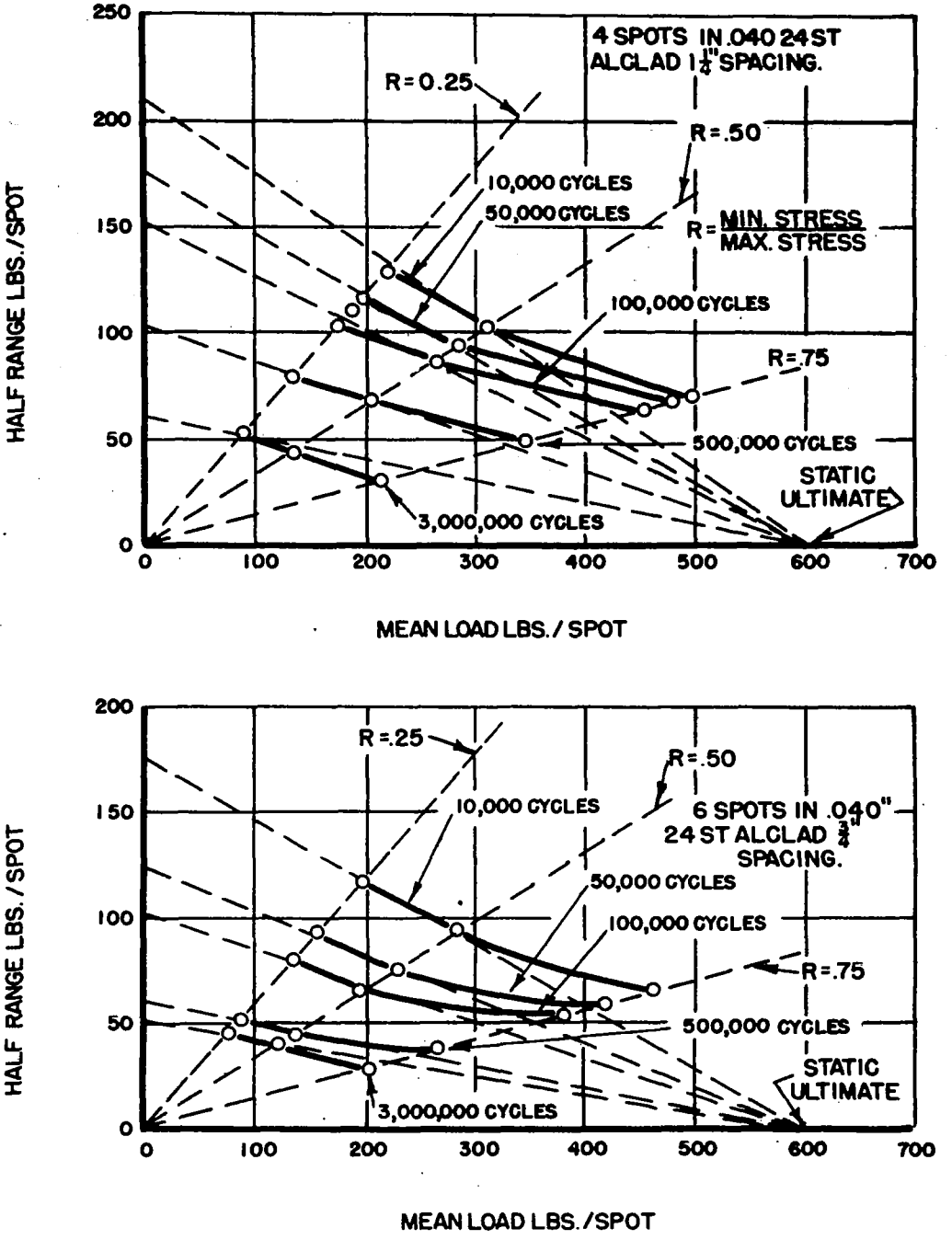

FIG. 15 – EFFECT OF MEAN LOAD ON FATIGUE STRESS RANGE ON SPOT WELDED LAP JOINTS IN .040" 24 ST ALCLAD SHEET.

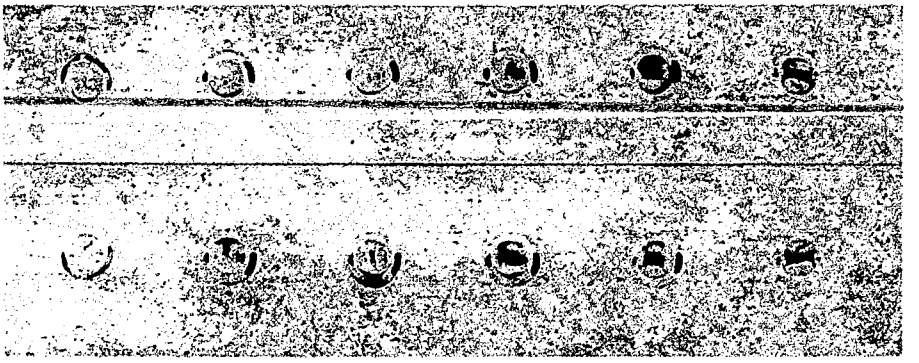

18074
1X

Figure 16.

Sample showing shear type failure through spots. Sample 3A - 4 (6).

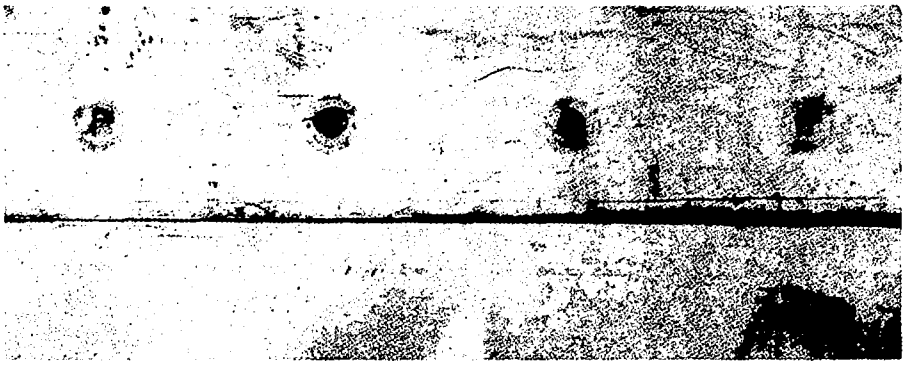

18070
1X

Figure 17.

Sample 3A - 14 (4) illustrating "button pulling" type of failure.

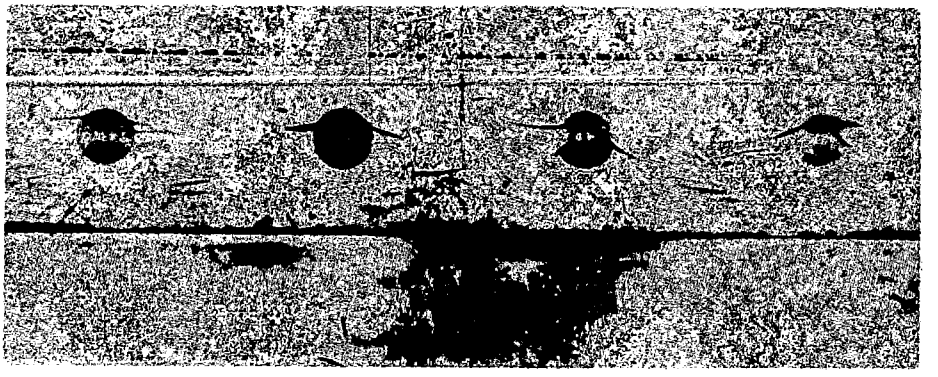

18071
1X

Figure 18.

Sample 3A - 29 (4) illustrating beginning of fatigue cracks at top of welds.

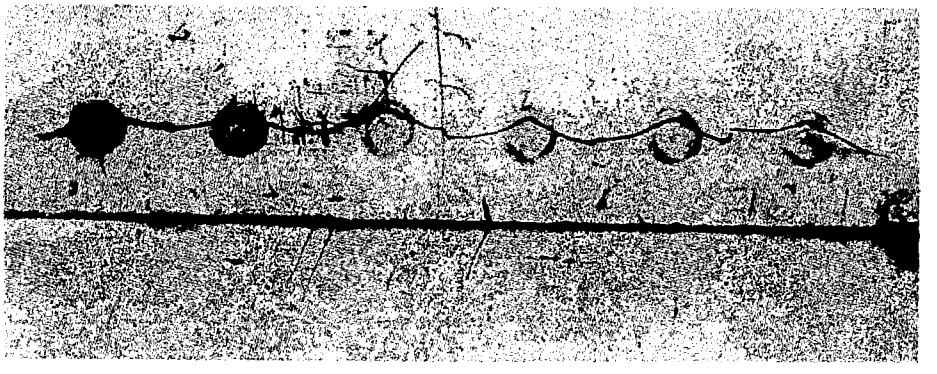

18072
1X

Figure 19.

Sample 3A -29 (6) showing propagation of fatigue cracks.

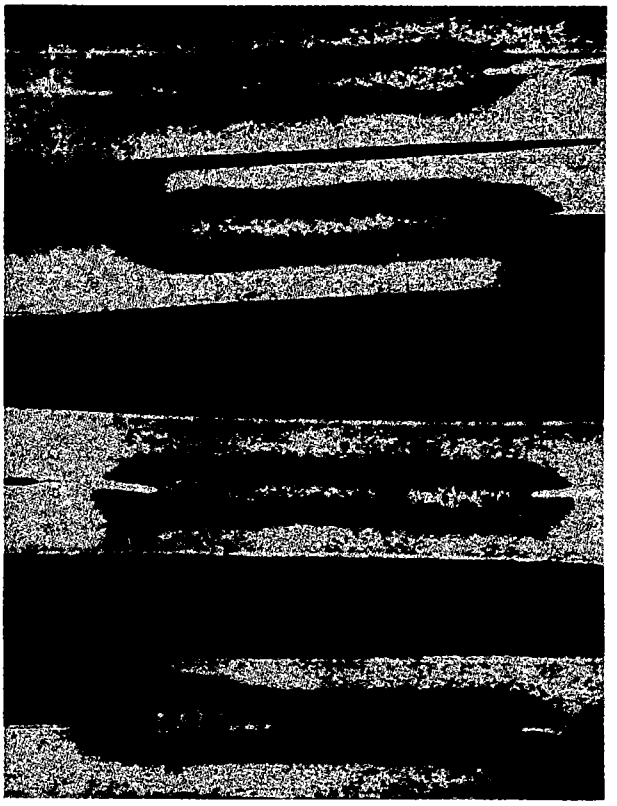

Kellers Etch
18277
10X

Figure 20.

0.040" - 0.040" 24S-T Alclad spotwelds in tensile specimen 3A23, sectioned both normal and parallel to direction of testing indicating failure only in direction of testing.

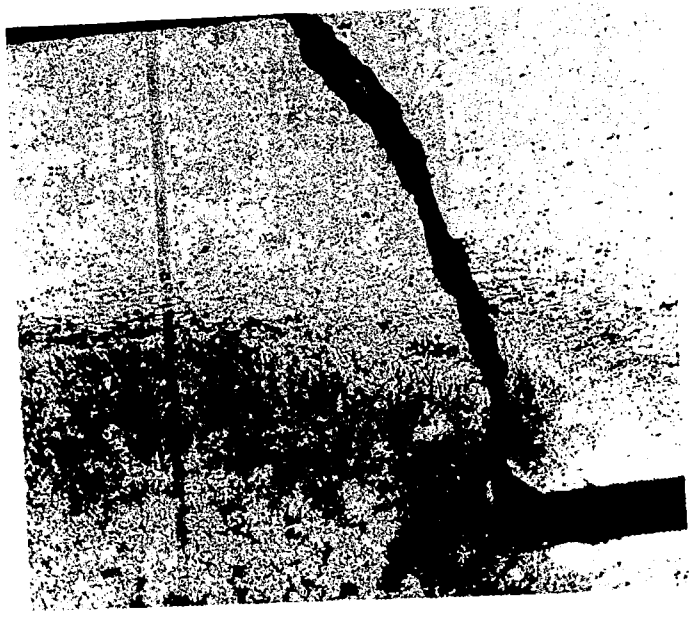

18273
75X
Kellers Etch

(a)

18278
10X

(b)

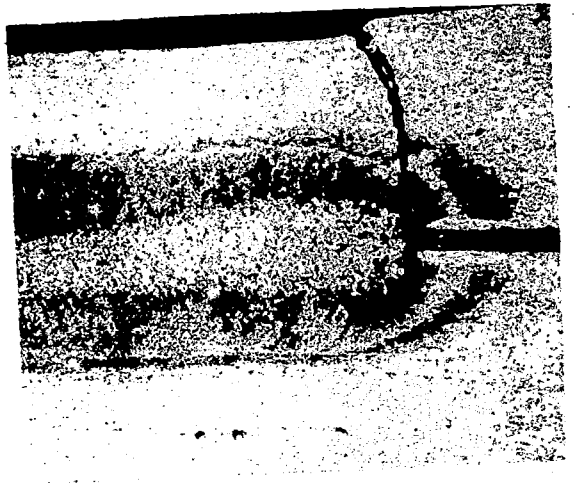

18272
25X
Kellers Etch

(c)

Figure 21.- 0.040" - 0.040" 24S-T Alclad spotweld in tensile specimen 3A25 showing typical fatigue failure under shear loading (sectioned parallel to stress application).

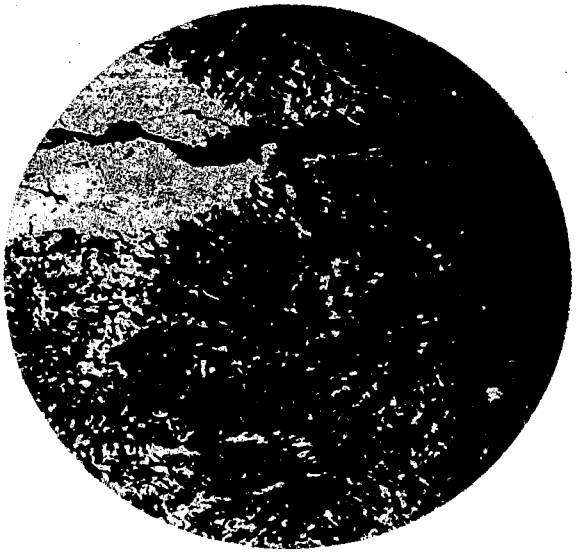

270 Kellers Etch
50X

(a)

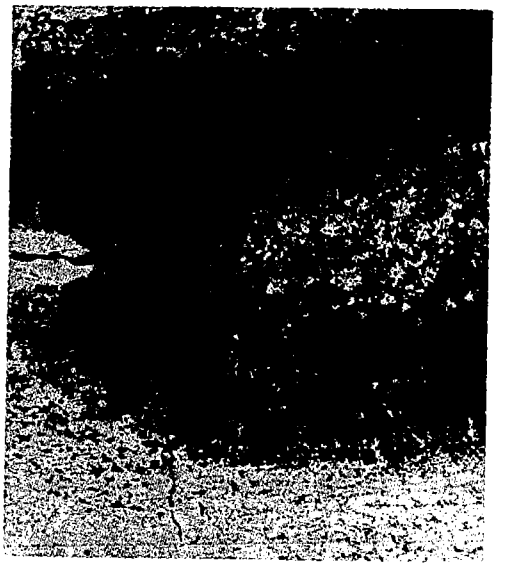

18271 Kellers Etch.
75X

(b)

Figure 22.

0.040" - 0.040" 24S-T Alclad spotwelds in tensile specimen 3A24 which has been subjected to over 3,000,000 cycles at light loading without failure, showing formation and propagation of fatigue crack from the notch formed by the Alclad projection into the spotweld. (Parallel sectioning.)

18266
75X

Kellers Etch

Figure 27

0.032" - 0.032" 24S-T Alclad spotweld in stiffened compression sample A8 sectioned normal to direction of testing. Parallel cracks indicated here occur only in close spotweld spacing.

Kellers Etch

18267
75X

Figure 23.

Untested spotweld in 0.040" - 0.040" 24S-T Al tension specimen showing elongated piping in area of Alclad projection.

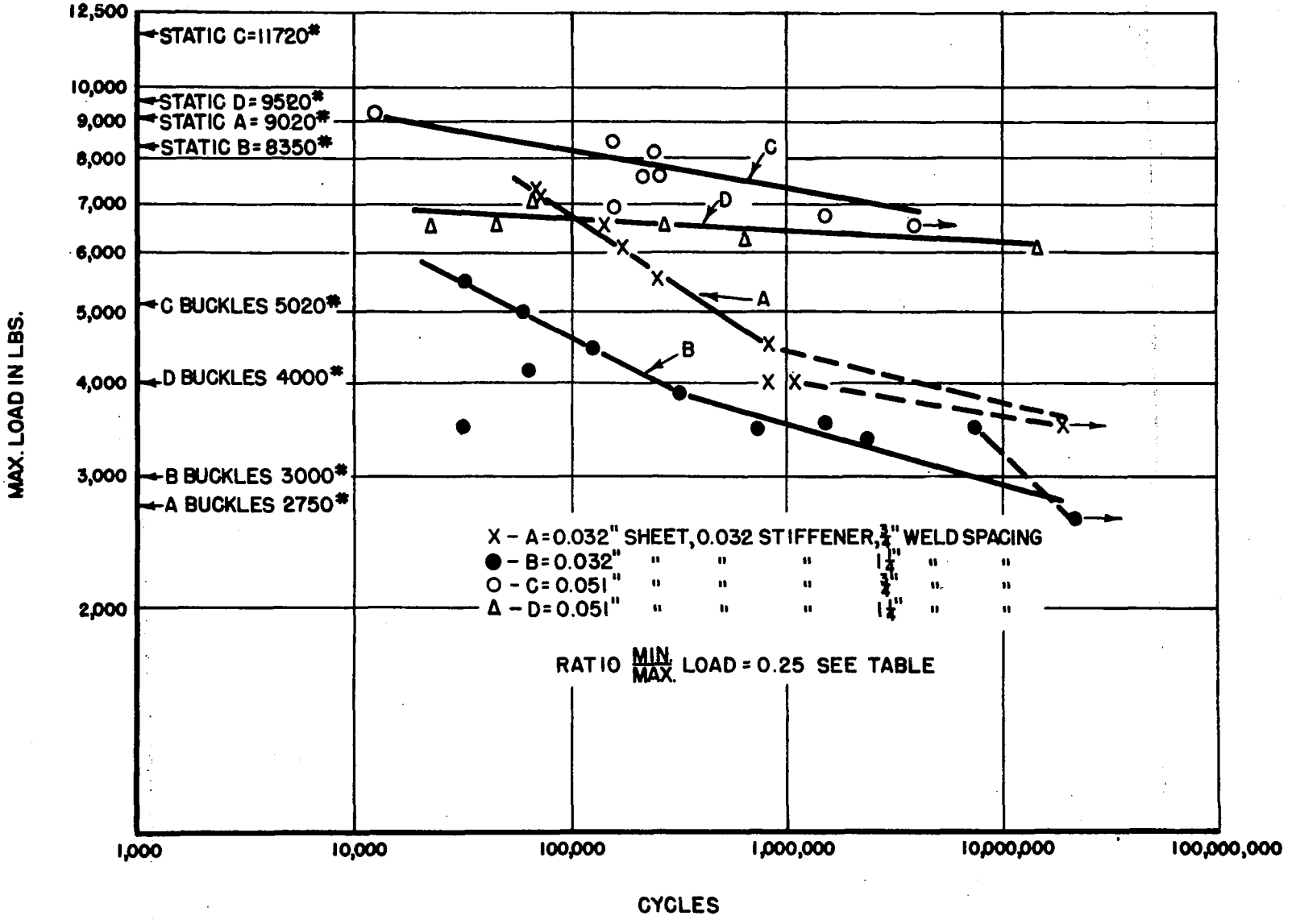

FIG. 24—COMPRESSION FATIGUE TESTS ON STIFFENED PANELS.

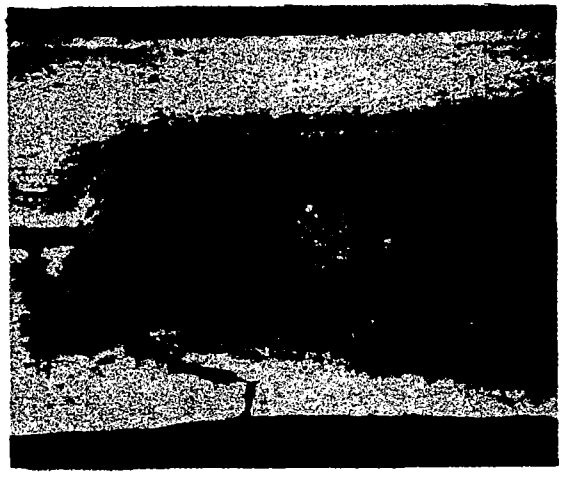

18268 Kellers Etch
25X

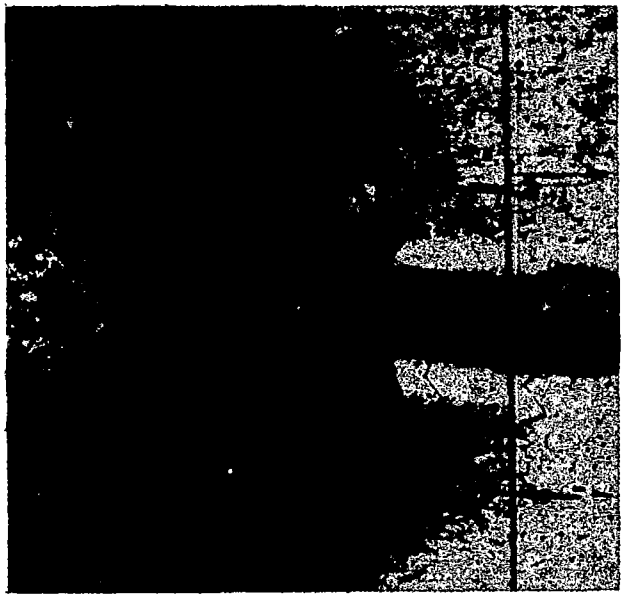

18269 Kellers Etch
75X

Figure 25.- Two views of 0.032"- 0.032" 24S-T Al spotweld in stiffened compression sample B4 next to break-sectioned parallel to direction of stress application. Note: Fatigue crack in sheet caused by nick in Alclad.

Figure 25a

Left hand side of weld.

Figure 25b

Right hand side of weld.

(a)

(b)

(c)

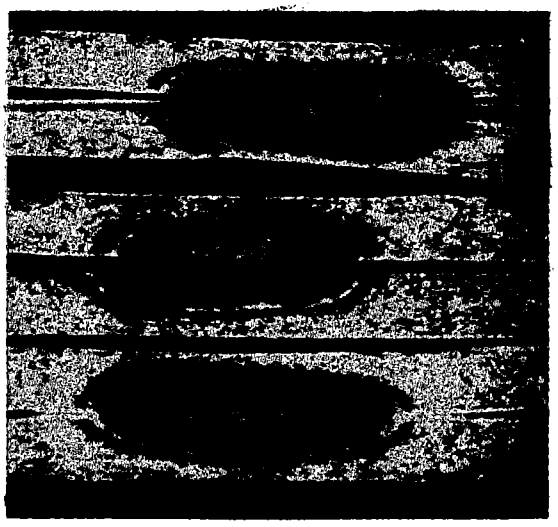

Kellers Etch 18230
10X

Figure 26

0.032" - 0.032" 24S-T Alclad Spotweld in stiffened compression sample B4.

(a) Next to break and sectioned parallel to direction of testing.

(b) Next of break and sectioned normal to direction of testing.

(c) Two welds from break and sectioned parallel to direction of testing.